A class of expansion functions for finite elastic plates in structural acoustics

Richard V. Craster
Department of Mathematics, Imperial College of Science, Technology and Medicine, London SW7 2BZ, United Kingdom

Stefan G. Llewellyn Smith
Department of Mechanical and Aerospace Engineering, University of California, San Diego, 9500 Gilman Drive, La Jolla, California 92093-0411

(Received 4 February 1999; accepted for publication 26 August 1999)

Problems in structural acoustics involving finite plates can be formulated using integral equation methods. The unknown function within the integral equation must satisfy the plate edge conditions, and hence appropriate expansion functions must be used. The expansion functions developed here are aimed at treating a wide class of problems. Once such functions are found, the solution process and numerical implementation are relatively straightforward. The speed of convergence to ''exact'' comparison solutions is fast even in the singular limit of high frequencies and wide plates. A set of expansion functions with the required properties is constructed and some illustrative problems are treated. © *1999 Acoustical Society of America.* [S0001-4966(99)03512-2]

PACS numbers: 43.20.Tb, 43.40.Dx, 43.40.Rj [CBB]

INTRODUCTION

Many papers have been written on integral equation methods for treating finite length rigid plates in acoustics, or analogous problems in elastodynamics or electromagnetism.[1,2] In these cases the integral equations are readily and efficiently solved using expansion functions, Chebyshev polynomials, for the unknown. The vital ingredient captured by the expansion functions is that they correctly incorporate the edge condition at the plate ends. Convergence is usually rapid even for higher frequency problems. Unfortunately, the usual Chebyshev polynomial expansion functions are not well suited to treating, say, elastic plate boundary conditions; the edge behavior is altered in these cases. Our aim here is to develop a class of expansion functions, analogous to the rigid plate ones, that are equally applicable to elastic plate problems.

There is recurrent interest in sound generation or scattering by elastic plates in structural acoustics. Many structures consist of plates welded together or attached in other ways, and vibrational plate waves are potential major sources of acoustic noise. These waves may be coupled into the surrounding fluid via interactions with the plate edges, for example. Thus analytical and numerical techniques have often been used to try to describe the general physical effects involved, and to solve model problems for specific geometries.[3] Problems involving finite length plates with various attachment conditions are unfortunately not amenable to exact solution, although asymptotic results for wide plates and light or heavy fluid loading can be found. Our aim is to develop efficient numerical approaches capable of solving these problems in regimes not necessarily amenable to asymptotic analysis, and which can also be generalized to more complex geometries.

In this paper we shall concentrate on a pedagogic two-dimensional example. However, the basis expansion functions we develop can be utilized in more complex geometries. From a numerical perspective one has to deal with a relatively high order boundary condition on the elastic plate, such as the classical plate equation,[4]

$$B\frac{\partial^4 \eta}{\partial x^4} - m\omega^2 \eta = -p(x,0), \tag{1}$$

for the plate displacement $\eta(x)$, where $p(x,0)$ is the pressure on the plate. This equation is adopted here and involves the fourth derivative of η. The plate is assumed to separate fluid from a vacuum. At any joint or plate edge we must apply two edge conditions to the displacement. For instance, clamped plates have $\eta=\eta'=0$ at the edges. The appropriate conditions must be built into any numerical scheme either implicitly or explicitly. Moreover, the edge conditions are important, as analytical studies show a marked dependence upon them.

A variety of numerical methods such as finite element schemes, modal methods, and integral equation approaches have been utilized by other authors. Finite elements are versatile. However, one has to discretize the whole domain, with the result that infinite domains are awkward, and calculations become increasingly unwieldy as frequencies increase. Modal methods have advantages for the simply supported $\eta=\eta''=0$ edge conditions, as Fourier series solutions can be developed; however, this approach cannot be used for more general edge conditions. For more general edge conditions, analytic approximations utilizing the *in vacuo* eigenfunctions can be adopted;[5] we briefly discuss eigenfunction methods in Sec. IV. There are also numerical approaches using the modified Wiener–Hopf technique;[6] these are perhaps less flexible than the numerical methods based directly upon solving the integral equations. Nonetheless they are formally exact if one continues the iterations indefinitely, although this is at the cost of considerable effort.

Integral equation methods have considerable advantages for relatively simple geometries, and this is the approach we develop here. Previous authors, for instance Mattei,[7] have adopted this technique, but have used different methods that have difficulties explicitly incorporating the edge conditions. Typically the edge conditions are treated separately, and since there have been few comparisons with exact or asymptotic methods, it is unclear how successful such numerical methods have been.

Here we treat the integral equations utilizing expansion functions that automatically take into account the edge conditions. As a result, the edge conditions are implicitly satisfied and no extra equations are required. This approach quickly leads to an accurate and efficient numerical scheme: typically only a few expansion functions are required to ensure accurate solutions. For plates with clamped edge conditions this approach has been detailed elsewhere,[8] and has been compared to asymptotic solutions near resonant frequencies and to asymptotic solutions for light and heavy fluid loading. Compliant plate effects are also easily treated and several types of forcings are considered: incident plane waves, line forces and moments, and sources in the fluid. Our aim previously[8] was to introduce and develop this approach and to show that it can be particularly useful in regimes not amenable to asymptotic analyses and hence convenient for quite general incident fields. The aim here is to expand upon the method and consider a wider class of edge condition.

We consider time harmonic vibrations of frequency ω, and all physical variables are assumed to have an $e^{-i\omega t}$ dependence. This is considered understood and is henceforth suppressed. Two-dimensional problems are considered with an inviscid, compressible fluid lying in $x_3>0$ and $-\infty<x_1<\infty$, and a vacuum lying in $x_3<0$. The fluid pressure $p(x_1,x_3)$ satisfies

$$(\nabla^2+k_0^2)p(x_1,x_3)=f(x_1,x_3), \tag{2}$$

where $f(x_1,x_3)$ corresponds to a distribution of fluid sources, and k_0, the acoustic wave number, is related to the sound speed c_0 via $k_0=\omega/c_0$. In what follows, the source distribution is zero except for Green's functions. The displacement in the x_3-direction within the fluid, $\eta(x_1,x_3)$, is related to the fluid pressure via

$$\rho\omega^2\eta(x_1,x_3)=\frac{\partial p(x_1,x_3)}{\partial x_3}. \tag{3}$$

The plane $x_3=0$ is taken to consist of a thin elastic plate in the finite region $|x_1|<a$ in which (1) holds, and to consist of a rigid plate elsewhere. The geometry is shown in Fig. 1.

The parameters B and m are the bending stiffness and mass per unit area of the plate, respectively. These parameters are related to the properties of the elastic plate via $B=Eh^3/12(1-\nu^2)$ and $m=\rho_s h$, with E, h, ν, and ρ_s the Young's modulus, plate thickness, Poisson ratio, and mass density of the elastic material, respectively. In order to minimize the number of parameters that occur later, we introduce the *in vacuo* flexural wave number $k_p\equiv(\omega^2 m/B)^{1/4}$. Incorporating a small loss factor will lead to attenuation of the plate waves; we shall not consider loss factors here. We introduce the nondimensional quantities[9] M and ϵ. The ''Mach'' number M is defined to be the ratio of the fluid sound speed to that of the *in vacuo* plate waves, $M\equiv k_0/k_p$. A frequency independent measure of fluid loading is provided by the parameter $\epsilon\equiv(B\rho^2/m^3c_0^2)^{1/2}$. In essence, when the system is lossless, there are three parameters that can be varied: M, ϵ, and k_0a, the last of these being the ratio of a typical length scale associated with the fluid disturbance to a typical length scale associated with the finite defect. Typically ϵ is small: for example, $\epsilon\approx0.134$ for steel plates in water, while M, which is frequency dependent, can range through all values. The fluid loading will be termed[9] ''light'' when $M\sim O(1)$, but is not in the immediate neighborhood of $M=1$, and ''heavy'' when $M\ll\epsilon$. In both cases ϵ is taken to be small, i.e., $\epsilon\ll1$.

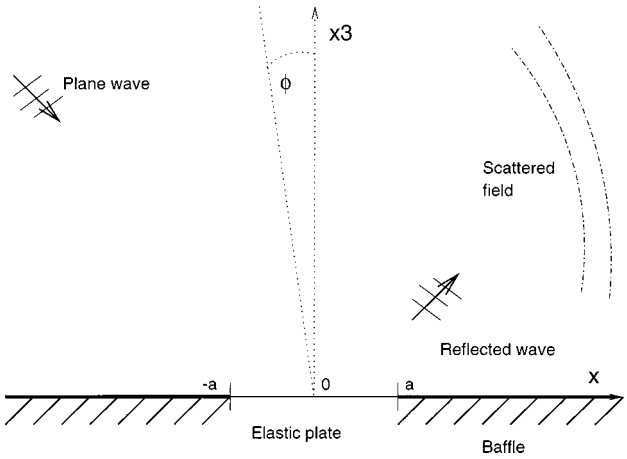

FIG. 1. Geometry of the problem. Note that $x\equiv x_1$, and that the two sets of Green's function variables in Sec. II are (x_1,x_3) and (q_1,q_3).

We previously treated the clamped edge conditions,[8] but there are other possibilities. Hinged plates satisfy the edge conditions $\eta=\eta''=0$ at their edges. The natural expansion functions in that case can be taken as the Fourier modes, $\cos\pi(n-1/2)x$, $n=1,2,\ldots$ and $\sin\pi nx$, $n=1,2,\ldots$. For the special case $\eta=\eta''=0$, we have used this approach for comparative purposes (see Sec. III), and to verify that our expansion functions are accurate in this case. We should emphasize that the Fourier modes are probably easier to use for this special case, but they cannot be used for the more general edge conditions (4) that we propose to tackle.

Leppington *et al.*[10] pointed out after looking at experimental data that a more realistic set of edge conditions might be

$$\eta''\pm\delta\eta'=0 \quad \text{at} \quad x=\pm1, \tag{4}$$

together with $\eta=0$ at $x=\pm1$, where δ is a positive number and the plate edges are at $x=\pm1$. The case $\delta=0$ corresponds to the hinged case, while the limit of large δ recovers the clamped case previously considered. The more general edge condition may be interpreted as a hinged edge with a restoring couple and may be incorporated into our approach by changing the previous expansion functions.[8]

The physical problem is split into pieces that are even and odd in x, and the superscripts $(e),(o)$ are used to denote

these subproblems. The even expansion functions are taken to be

$$\psi_n^{(e)}(x) = \begin{cases} \cos[n\ \cos^{-1}\{(1-x^2)(1-ax^2)\}] & \text{for } n \text{ odd}, \\ (1-x^2)\cos[(n-1)\cos^{-1}(1-x^2)^2] & \text{for } n \text{ even}, \end{cases} \tag{5}$$

in $0 \leqslant x \leqslant 1$. For negative x these are extended as even functions of x. The quantity a is given by

$$a = \frac{1+\delta}{5+\delta}. \tag{6}$$

The odd functions become

$$\psi_n^{(o)}(x) = \begin{cases} i\ \sin[(n+1)\cos^{-1}\{(1-x^2)(1-ax^2)\}] & \text{for } n \text{ odd}, \\ i(1-x^2)\sin[n\cos^{-1}(1-x^2)^2] & \text{for } n \text{ even} \end{cases} \tag{7}$$

in $0 \leqslant x \leqslant 1$. These are extended as odd functions of x for x negative. This choice of expansion functions is adopted as the expansion functions satisfy the edge conditions exactly; it is worth noting that these expansion functions are related to Chebyshev polynomials with the appropriate edge behavior in their argument. The expansion functions for n even are required, as the terms with n odd exclude the terms of the form $(1-x^2)^3$ near the edge, which also satisfy the edge conditions. As we shall see, these expansion functions extend those usually used for rigid plates, allowing one to extend previous analyses to elastic plates.

I. COMPLETENESS OF THE EXPANSION FUNCTIONS

One issue surrounding these expansion functions is whether they have any underlying mathematical basis. It is important to verify that the plate displacement can actually be represented by the expansion functions, and that the latter are hence complete. The expansion functions typically used in elasticity for crack problems[2] may easily be shown to be complete. These functions are (to within a normalization factor),

$$\phi_n(x) = \begin{cases} \cos(n\ \sin^{-1}x) & \text{for } n \text{ odd}, \\ \sin(n\ \sin^{-1}x) & \text{for } n \text{ even}, \end{cases} \tag{8}$$

on the interval $(-1,1)$. Both the even and odd functions of x can be conveniently considered together. The change of variable $x = \sin\theta$ maps the x-interval $(-1,1)$ onto the θ-interval $(-\pi/2, \pi/2)$. On this interval, the expansion functions are

$$\phi_n = \begin{cases} \cos n\theta & \text{for } n \text{ odd}, \\ \sin n\theta & \text{for } n \text{ even}. \end{cases} \tag{9}$$

This set of functions is complete on the interval $(-\pi/2, \pi/2)$, since it corresponds to the usual Fourier sine expansion on the interval.

The set given by (5)–(7) requires more care.[8] Any function f on $(-1,1)$ may be decomposed into its odd and even parts f_o and f_e, respectively, both defined on (0,1) and with $f_e'(0) = f_o(0) = 0$. The change of variable $\cos\theta = (1-x^2)(1-ax^2)$ is a one-to-one and onto mapping of the x-interval (0,1) onto the θ-interval $(0, \pi/2)$. On this new interval, the transformed even expansion functions are again $\cos n\theta$ for n odd. However, the expansion functions are not complete on this interval: a complete set of trigonometric functions for the expansion of even functions on this interval requires even n as well. One cannot just add the even cosines as extra expansion functions though, since this would remove the correct edge condition in the original variable x and hence introduce Gibbs' effects that would undermine the whole aim of the expansion functions. The additional functions $\psi_e' = (1-x^2)\cos[n\cos^{-1}(1-x^2)^2]$, which explicitly introduce terms of the form $(1-x^2)^3$ near $x = \pm 1$, satisfy the appropriate edge conditions, and project onto all the cosine functions, in particular onto the even ones. This was shown for the clamped case previously.[8] Hence the set of expansion functions for the even part of f is complete. The issue of whether these expansion functions are orthogonal with respect to a particular weight function is irrelevant since orthogonality properties are never used.

The argument for the odd part of f is analogous. Therefore the set of expansion functions (5)–(7) is complete, and in addition satisfies the appropriate edge conditions.

II. FORMULATION AND SOLUTION OF INTEGRAL EQUATIONS

We consider the plane $x_3 = 0$ with the elastic plate lying on $|x_1| < a$ and a rigid baffle on $|x_1| > a$. As can be shown from a Green's function approach, the scattered pressure field at a point (q_1, q_3) is given by

$$p^{sc}(\mathbf{q}) = -\rho\omega^2 \int_{-a}^{a} \eta^{sc}(x_1,0) p^G(x_1,0;\mathbf{q})\, dx_1, \tag{10}$$

where $p^G(\mathbf{x},\mathbf{q})$ is the Green's function for (2) which has vanishing x_3-derivative in $x_3 = 0$. The plate displacement $\eta^{sc}(x_1,0)$ is unknown in (10) and our aim is to identify this function in the most efficient manner. Once this is identified the problem is effectively solved, since pressure fields and far-field behavior follow directly from (10). Hence we concentrate upon whether we have identified η correctly, and our comparisons with other techniques are based upon this quantity.

The Green's function is the inverse Fourier transform

$$p^G(\mathbf{x};\mathbf{q}) = \frac{i}{4\pi} \int_C \frac{1}{\gamma_0} [e^{i\gamma_0|x_3-q_3|} + e^{i\gamma_0(x_3+q_3)}] e^{ik(x_1-q_1)}\, dk, \tag{11}$$

which also has a representation in terms of Hankel functions. The path C runs along the real axis suitably indented at the branch points $\pm k_0$. The function $\gamma_0 = (k_0^2 - k^2)^{1/2}$ has a positive imaginary part. An advantage of persisting with a transform based representation is that for more complex geometries the Green's functions emerge in a similar manner; the approach that is required follows that presented here.

As it stands, (10) is not in the form where we can solve for the unknown displacement, since the left-hand side is also unknown. To remedy this, we manipulate (10) so that

the left-hand side becomes the plate equation, and we are left with an integral equation to solve. The manipulation is most easily performed by replacing $p^G(x_1,0;\mathbf{q})$ in (10) with its transform (11) and applying the operator D_q defined by

$$D_q = B\partial_{q_1}^4 - m\omega^2, \tag{12}$$

where the notation $\partial_{q_i} = \partial/\partial q_i$ has been adopted. Thus we obtain

$$p^{sc}(q_1,0) + D_q \eta^{sc}(q_1,0) = \frac{B}{2\pi}\int_{-a}^{a} \eta^{sc}(x_1,0)\, dx_1 \times \int_{-\infty}^{\infty}\left[k^4 - \frac{m\omega^2}{B} - \frac{i\omega^2\rho}{\gamma_0 B}\right] e^{ik(x_1-q_1)}\, dk \tag{13}$$

for $|q_1|<a$.

Two types of forcing can be adopted here: either incident waves or local plate excitation. We treat the incident wave case in detail, in which case the left-hand side in the above equation is equal to $-(p^{in}+D_q\eta^{in})$. For plane wave incidence, the incident and reflected pressure wave together are

$$p^{in}(q_1,q_3) = A[e^{i(kq_1+\gamma_0 q_3)} + e^{i(kq_1-\gamma_0 q_3)}], \tag{14}$$

where

$$k = k_0 \sin\theta_i \tag{15}$$

is the incoming wave number. This corresponds to the field produced by a pressure wave incident upon a defect-free rigid plate. The incident displacement field therefore vanishes on the elastic plate, leading to

$$-[p^{in}+D_q\eta^{in}](q_1,0) = -2Ae^{ikq_1} \tag{16}$$

for $|q_1|<a$.

Each applied incident field is split into two subproblems, one that is even in x, and one that is odd in x. The unknown displacement along the plate is expanded in terms of the expansion functions (5)–(7). The appropriate expression, in which the factor $4a^4/B$ is inserted for convenience, is

$$\eta^{sc}(x_1,0) = \frac{4a^4}{B}\sum_{n=1}^{\infty}(a_n^{(e)}\psi_n^{(e)}(x_1/a) + a_n^{(o)}\psi_n^{(o)}(x_1/a)). \tag{17}$$

The integral equation (13) is split into even and odd subproblems. The even subproblem is then solved by multiplying (13) by $\psi_m^{(e)}(q_1/a)$ and integrating from $-a$ to a, as well as expanding the scattered displacement on the plate, leading to

$$-\pi A\int_{-1}^{1}\cos(kaq_1)\psi_m^{(e)}(q_1)\, dq_1 = \sum_{n=1}^{\infty} a_n^{(e)}\int_{-\infty}^{\infty}\int_{-1}^{1}\int_{-1}^{1}\psi_m^{(e)}(q_1)\psi_n^{(e)}(x_1)e^{il(x_1-q_1)} \times\left[l^4 - (ak_p)^4 - \frac{i(ak_p)^6\epsilon}{ak_0[(ak_0)^2-l^2]^{1/2}}\right] dx_1\, dq_1\, dl\,. \tag{18}$$

The procedure for the odd subproblem is identical. The governing equation (18) may be rewritten as an infinite set of linear equations

$$b_m^{(e)}(ka) = \sum_{n=1}^{\infty} K_{mn}^{(e)} a_n^{(e)}, \tag{19}$$

for $m=1,\ldots,\infty$, where the left-hand side terms, which depend on the incident wave number, are given by

$$b_m^{(e)}(ka) = -\pi A\int_{-1}^{1}\cos(kaq_1)\psi_m^{(e)}(q_1)\, dq_1 \tag{20}$$

for incident plane waves; the counterpart for the odd subproblem follows in a similar manner. The right-hand side factors are given by

$$K_{nm}^{(e)} = I_{mn}^{(e)(1)} - (ak_p)^4 I_{mn}^{(e)(2)} - i(ak_p)^6\epsilon I_{mn}^{(e)(3)}/ak_0\,. \tag{21}$$

Truncating this set of equations, and its counterpart for the odd subproblem, at some finite order N will give an approximate, but arbitrarily accurate (depending on the order of the truncation) solution to the original problem. Noting the symmetry with respect to m and n means that even for relatively large N, one need not evaluate an undue number of the K_{mn}.

We consider each term in K_{mn} in succession, dropping the superscripts. The corresponding pieces of the triple integral are

$$I_{mn}^{(1)} = 2\pi\int_{-1}^{1}\psi_m''(x_1)\psi_n''(x_1)\, dx_1 + 2\pi\delta[\psi_m'(1)\psi_n'(1) + \psi_m'(-1)\psi_n'(-1)]. \tag{22}$$

The last two terms of this expression are zero in the limiting cases of clamped or hinged edge conditions. The second integral leads to

$$I_{mn}^{(2)} = 2\pi\int_{-1}^{1}\psi_m(x_1)\psi_n(x_1)\, dx_1\,, \tag{23}$$

and the third integral is

$$I_{mn}^{(3)} = \pi\int_{-1}^{1}\int_{-1}^{1}H_0^{(1)}(k_0a|x_1-q_1|)\psi_m(q_1)\psi_n(x_1)\, dx_1\, dq_1\,. \tag{24}$$

These are all relatively simple to evaluate numerically. The above could also be deduced directly from the boundary condition, but it is perhaps more natural to proceed from the integral equation. This approach is more readily adjusted to deal with other geometries.

As noted earlier, once we have the displacement we can use (10) to deduce the pressure fields. The far-field behavior of the scattered field is obtained by expanding the double integral in (10) [note the Green's function in (10) is itself an integral] for large $|\mathbf{q}|$. Taking the far-field variable as

$$\mathbf{q} = r(-\sin\phi, \cos\phi), \tag{25}$$

and using a steepest-descents approach, gives

$$p^{sc}(r,\phi) \sim \left(\frac{2}{\pi r k_0}\right)^{1/2} G(\phi)e^{i(k_0 r - \pi/4)} \tag{26}$$

for $k_0 r \gg 1$. In the even subproblem this is

$$G^{(e)}(\phi) = -\frac{2i(k_p a)^6}{(k_0 a)} \epsilon \sum_{n=1}^{\infty} a_n^{(e)} \times \int_{-1}^{1} \psi_n^{(e)}(x_1) \cos(a k_0 x_1 \sin \phi) dx_1 . \quad (27)$$

A similar expression holds for the odd subproblem (replacing the cosine with a sine). The total directivity $G(\phi)$ is the sum of the even and odd expressions. The coefficients $a_n^{(e)}$ depend on the type of forcing adopted, and are the solutions of (19). The directivity is hence specified entirely by the a_n, as is the plate displacement. However, the latter quantity is simpler to compare to asymptotic approximations that we will develop and we shall hence concentrate on it.

III. ASYMPTOTIC RESULTS FOR LIMITING CASES

To demonstrate the accuracy of the above numerical scheme we compare it with various light fluid loading results. In the absence of fluid loading one can solve the plate equation, to get, for instance in the case of an incoming wave, the plate displacement

$$\eta^{sc}(x_1,0) = \frac{2A}{B(k_p^4 - k^4)} \left\{ e^{ikax} + [\delta(ka \cos k_p a \sin ka - k_p a \sin k_p a \cos ka) - \cos k_p a \cos ka\{(k_p a)^2 - (ka)^2\}] \times \frac{\cosh k_p a x}{k_p a D(k_p a)} + [\delta(ka \cosh k_p a \sin ka - k_p a \sinh k_p a \cos ka) - \cosh k_p a \cos ka\{(k_p a)^2 + (ka)^2\}] \times \frac{\cos k_p a x}{k_p a D(k_p a)} + [\delta(k_p a \cos k_p a \sin ka - ka \sin k_p a \cos ka) + \sin k_p a \sin ka\{(k_p a)^2 - (ka)^2\}] \frac{i \sinh k_p a x}{k_p a F(k_p a)} + [\delta(ka \sinh k_p a \cos ka - k_p a \cosh k_p a \sin ka) - \sinh k_p a \sin ka\{(k_p a)^2 + (ka)^2\}] \frac{i \sin k_p a x}{k_p a F(k_p a)} \right\}, \quad (28)$$

where the denominators, which are related to resonances of the system, are

$$D(k_p a) = \delta(\cosh k_p a \sin k_p a + \sinh k_p a \cos k_p a) + 2 k_p a \cosh k_p a \cos k_p a, \quad (29)$$

$$F(k_p a) = \delta(\sinh k_p a \cos k_p a - \cosh k_p a \sin k_p a) - 2 k_p a \sinh k_p a \sin k_p a. \quad (30)$$

This, and the corresponding far-field directivity, are reproduced by the numerics. As noted earlier, the case $\delta = 0$, corresponding to edge conditions $\eta = \eta'' = 0$, is amenable to Fourier analysis (although $\delta \neq 0$ is not). Hence we are independently comparing the performance of the expansion functions. Figure 2 shows the absolute error in the real part of the plate displacement for $k_0 a = 25$ and $\delta = 0$, which corresponds to a wide plate, as well as the error for the solution calculated by a sum in Fourier modes. The present procedure converges quickly to the exact answer more quickly than the Fourier expansion. This is a consequence of the well-known properties of the Chebyshev polynomial approximation. For this specific edge condition, $\eta = \eta'' = 0$, we are not necessarily suggesting that Fourier modes are of little value—they are very simple to deal with numerically—but merely aim to demonstrate that the expansion functions we propose are accurate in this special case.

The formula (28) fails near zeros of $D(k_p a)$ or $F(k_p a)$. In this limit one can proceed to get asymptotic results using eigenfunction methods, or via a wide strip approximation and the Wiener–Hopf technique. A simpler approximation, at least for $M > 1$, is to replace the plate equation (1) by

$$B\left(\frac{\partial^2}{\partial x^2} - k_l^2\right)\left(\frac{\partial^2}{\partial x^2} - \mu^2\right) \eta(x) = -p^{\text{inc}}. \quad (31)$$

The complex wave numbers k_l, μ are perturbations away from k_p and ik_p, respectively. For $\epsilon \ll 1$, the k_l are the leaky zeros corresponding to the leaky waves in the physical domain; they are in close proximity to the *in vacuo* wave numbers $\pm k_p$. The other wave numbers are at $\pm \mu$; these are in the proximity of $\pm i k_p$ and lead to rapidly decaying modes. If $M > 1$ these are given by the approximations[11]

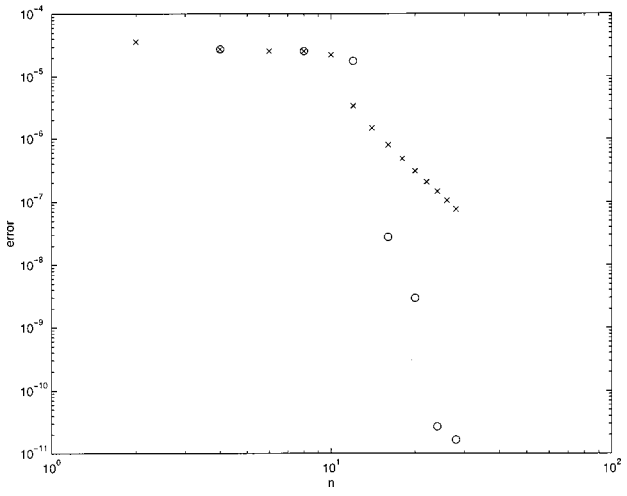

FIG. 2. Absolute error in the infinity norm of the real part of the plate displacement vs n, the order of truncation, for $k_0 a = 25$, $M = 1.5$, $\theta_i = 0$, $\epsilon = 0$, and $\delta = 0$. The circles show the error for the present scheme. The crosses show the error for the expansion in Fourier modes. Both circles and crosses are plotted for each value of n at which more resolution is achieved.

$$\mu \sim k_p\left(i-\frac{\epsilon}{4M(M^2+1)^{1/2}}\right), \tag{32}$$

$$k_l \sim k_p\left(1+\frac{i\epsilon}{4M(M^2-1)^{1/2}}\right); \tag{33}$$

otherwise they may be found numerically as the appropriate zeros of $k^4-k_p^4+\epsilon k_p^6/ik_0\gamma_0(k)=0$. This equation also has two real zeros, but these do not significantly affect the results in this light fluid loading limit. Thus this approximation assumes that the acoustic coupling is completely captured within the modified wave numbers. As shown[8] via a comparison with more rigorous methods, this is not quite true (particularly for $M<1$), but for practical purposes it does provide accurate solutions.

For brevity we will look at a wide strip approximation. For a wide strip we can deal with each plate edge independently and then look at the effect of the diffracted by one edge upon the other and vice-versa. This allows the natural separation of the problem into a sequence of semi-infinite problems which can be solved exactly using the Wiener–Hopf technique. However, it is much easier to use (31), and this has been justified previously.[8] For normally incident plane waves one finds that

$$\eta(x,0)\sim \frac{2}{B(k_p^4(1+i\epsilon k_p^2/k_0^2)}\left(1+\frac{(\mu^2+i\mu\delta)\cos\, k_l x_1-2(k_l^2\,\cos^2 k_l a+\delta k_l\,\sin\, k_l a)\,\cos\,(\mu x_1)e^{i\mu a}}{(k_l^2\,\cos\, k_l a+\delta k_l\,\sin\, k_l a)-(\mu^2+i\delta\mu)\cos\, k_l a}\right). \tag{34}$$

More explicit results showing the dependence upon ϵ, for $M>1$, are obtained by substituting the zeros (33) into (34). At resonance, the displacement (and far-field directivity) is $O(1/\epsilon)$ rather than $O(1)$. For instance, in the simplest case, $\delta=0$, the resulting displacement is

$$\eta(x,0)\sim \frac{2i}{Bk_p^4}(-1)^{n+1}\cos\left(\left(n+\frac{1}{2}\right)\pi\frac{x}{a}\right)\frac{2M(M^2-1)^{1/2}}{\epsilon k_p a}, \tag{35}$$

for $k_p a=(n+1/2)\pi$. The plate displacements found near a resonance for $\epsilon=0.134$, $k_0a=7.209$, $M=1.5$,and $\delta=1$ are shown, normalized by a factor B/a^4 in Fig. 3.

Strictly, the approximation holds for $\epsilon\ll 1$ (and for $M>1$). However it still appears to give good results for relatively large ϵ, such as 0.134 with the accuracy improving as ϵ decreases. In any case, for our purposes, it provides a useful confidence check upon the numerical results.

The plate displacements found for $\delta=0$, $\epsilon=0.134$, $k_0a=11.781$, and $M=1.5$ are shown, normalized by a factor B/a^4 in Fig. 4. The approximation (35) is also shown.

Once the plate displacements are found, the directivities follow from

$$G(\phi)=\frac{\rho\omega^2}{2i}\int_{-a}^{a}\eta(x,0)e^{ik_0x\,\sin\,\phi}\,dx, \tag{36}$$

and there is close agreement between the numerical and asymptotic results. All numerical work is also checked utilizing power balance and reciprocity relations.[8]

IV. EIGENFUNCTION EXPANSIONS

The set of expansion functions we have utilized is not the only one that could be used. Indeed one could use any complete set that satisfied the edge conditions. Clearly, an alternative candidate set consists of the eigenfunctions asso-

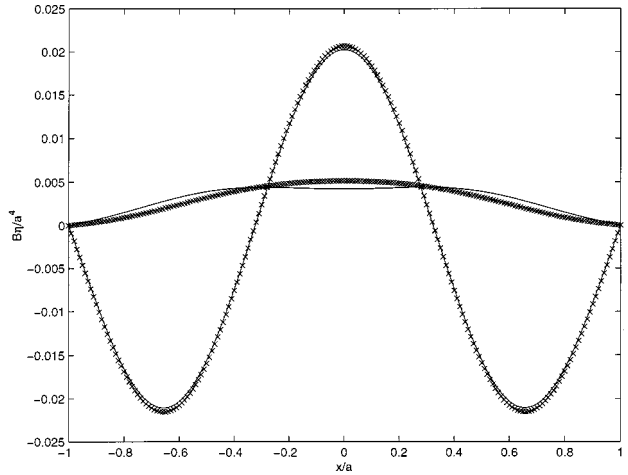

FIG. 3. Real and imaginary parts of the plate displacement $B\eta^{sc}(x,0)/a^4$: solid lines are the numerical solution (the imaginary part is the larger one), crosses are the analytical solution (28) vs x/a for $k_0a=7.209$, $M=1.5$, $\theta_i=0$, $\epsilon=0.134$, and $\delta=1$.

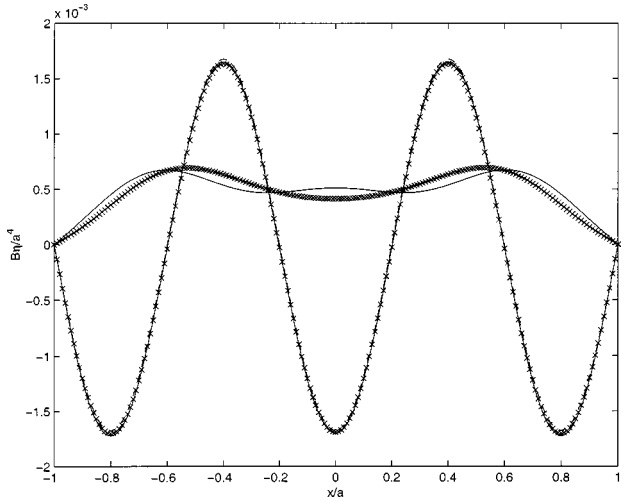

FIG. 4. Real and imaginary parts of the plate displacement $B\eta^{sc}(x,0)/a^4$ (solid lines and crosses as in Fig. 3 with the imaginary part again having larger magnitude) vs x for $k_0a=11.781$, $M=1.5$, $\theta_i=0$, $\epsilon=0.134$, and $\delta=0$. The dashed line shows the imaginary part of (35).

ciated with the *in vacuo* plate displacements. For example, for the special case of clamped edge conditions with even loadings, we could try

$$\eta^{sc}(x,0)=\frac{4a^4}{B}\sum_{n=1}^{\infty} a_n(\cos\lambda_n x\,\sinh\lambda_n+\sin\lambda_n\,\cosh\lambda_n x), \tag{37}$$

where the eigenvalues λ_n are the consecutive zeros of the transcendental equation

$$\sinh\lambda_n\cos\lambda_n+\sin\lambda_n\cosh\lambda_n=0. \tag{38}$$

These are easily found using the approximate zeros $\lambda_n=\pi(n-1/4)$, $n=1,2,\ldots$ as the initial values in a Newton–Raphson scheme. These expansion functions satisfy the edge conditions exactly, and moreover they are orthogonal. There is no reason why these cannot be used as expansion functions in an identical manner to that which we have adopted in earlier sections, and indeed for comparative purposes we have done that. We have found these less flexible than the set of expansion functions we have developed, primarily because the expressions become more unwieldy, particularly for general δ and general loadings [(37) is just for the clamped case with even loading]. They are not easily carried across to three-dimensional problems, whereas the simpler sine and cosine functions are easy to program in. In addition, the eigenfunctions will not have the desirable features of Chebyshev approximation of the expansion functions we have developed. As our aim is to provide simple and flexible expansion functions we prefer not to use the *in vacuo* eigenfunctions. In addition, for heavy fluid loading these are not convenient expansion functions, as in that case, in rescaled coordinates, the structural inertia [the k_p^4 terms in the plate equation (1)] vanishes to leading order. Thus it is felt that a set of expansion functions satisfying the edge conditions exactly, but not tied in too closely with one piece of the boundary condition, is more flexible.

V. CONCLUSION

A fast, efficient, and flexible numerical scheme capable of dealing with a variety of plate edge conditions is presented; this is an extension of a technique often used for rigid plates. We focus on determining the plate displacement, as all other details can ultimately be determined from this quantity. Clearly it is important to verify that this class of expansion functions produces accurate results, particularly near resonance. To verify accuracy, the numerical results are compared with asymptotic results for light fluid loading, both near to, and far from, resonance. The results are also compared with a Fourier analysis of the special case of simply supported edges. Further numerical results for the clamped edge condition can be found in Ref. 8. The scheme for the more general edge conditions we have discussed here has similar accuracy and versatility.

A useful approximation (34) for light fluid loading, based upon varying the *in vacuo* wave number is also highlighted. Good agreement was found in all cases.

ACKNOWLEDGMENTS

S.G.L.S. was funded by a Lindemann Trust Fellowship administered by the English Speaking Union during the duration of this work, which was carried out at the Scripps Institution of Oceanography. R.V.C. acknowledges the support of an EPSRC Advanced Fellowship.

[1] J. D. Achenbach and Z. L. Li, Wave Motion **8**, 225–234 (1986).
[2] F. L. Neerhoff and J. H. M. T. van der Hijden, J. Sound Vib. **93**, 523–536 (1984).
[3] D. G. Crighton, A. P. Dowling, J. E. Ffowcs Williams, M. Heckl, and F. G. Leppington, *Modern Methods in Analytical Acoustics* (Springer, New York, 1992).
[4] M. C. Junger and D. Feit, *Sound, Structures and their Interaction*, 2nd ed. (Acoustical Society of America, Westwood, 1986).
[5] F. G. Leppington, Q. J. Mech. Appl. Math. **29**, 527–546 (1976).
[6] J. F. M. Scott, Philos. Trans. R. Soc. London, Ser. A **338**, 145–167 (1992).
[7] P. O. Mattei, J. Sound Vib. **179**, 63–77 (1995).
[8] S. G. Llewellyn Smith and R. V. Craster, Wave Motion **30**, 17–41 (1999).
[9] D. G. Crighton and D. Innes, J. Sound Vib. **91**, 293–314 (1983).
[10] F. G. Leppington, E. G. Broadbent, and K. H. Heron, Proc. R. Soc. London, Ser. A **393**, 67–84 (1984).
[11] D. G. Crighton, J. Sound Vib. **63**, 225–235 (1979).